



Properties of Indium Doped Zinc Oxide Thin Films Deposited by RF Magnetron Sputtering

Joon Ho Bang^a, Se Hun Park^a, Sang Hyun Cho^b, Pung Keun Song^{a*}

^aDepartment of Materials Science and Engineering, Pusan National University, Busan 609-735, Korea

^bNano Convergence Practical Application Center, Daegu Technopark

(Received August 29, 2010; revised August 29, 2010; accepted August 30, 2010)

Abstract

Indium doped zinc oxide films (ZIO) were deposited on non-alkali glass substrates by radio frequency (RF) magnetron sputtering at room temperature. The structural, electrical and optical properties of the ZIO films were investigated as a function of their In₂O₃ content (3.33-15.22 wt%). The ZIO films deposited with an In₂O₃ content of 9.54 wt% showed a relatively low resistivity of $9.13 \times 10^{-4} \Omega\text{cm}$ and a highly *c*-axis preferred orientation. The grain size and FWHM were mainly affected by the In₂O₃ content. The crystallinity and resistivity were enhanced with increasing grain size. The average transmittance of the ZIO films was over 85% in the visible region and their band gap varied from 3.22 to 3.66 eV depending on their doping ratio.

Keywords: ZnO, ZIO, TCO, RF magnetron sputtering

1. Introduction

Transparent conducting oxide (TCO) films with an optical transmittance exceeding 80% in the visible region and a low resistivity have been widely used in a variety of applications until now¹⁾. Recently, TCO films have become the subject of intense investigation for use as transparent electrodes in optoelectric devices such as flat panel displays (FPDs), solar cells, infrared (IR) reflectors and organic light-emitting diodes (OLED). Most of the previous research on TCOs has been focused on indium tin oxide (ITO). However, TCO films based on zinc oxide (ZnO) have also received much attention, due to their advantages such as non toxicity, low cost and the relative abundance of this material^{2,3)}. Furthermore, ZnO-based TCO films are more resistant to reductive hydrogen plasmas than In₂O₃-based films. TCO films can be prepared by a variety of techniques such as DC magnetron sputtering, RF magnetron sputtering, chemical vapor deposition (CVD), pulsed-laser deposition (PLD), molecular beam epitaxy (MBE)

and spray-pyrolysis⁴⁾. Normally, stoichiometric non-doped ZnO films present a high resistivity, due to their low carrier density. Therefore, Group III donor elements, such as Al, B, Ga and In, are added to improve the electrical properties of ZnO films. These high-valence metal elements can be regarded as the donor, which replaces the Zn atoms of the ZnO matrix⁵⁾. As a result, one electron is freed up to contribute to the electrical conductivity. Among the various zinc based TCOs, Al doped (AZO) and Ga doped ZnO (GZO) films have been extensively studied in recent years. Compared with AZO and GZO, there are few reports on In doped ZnO (ZIO).

2. Experimental

ZIO films were deposited on non-alkali glass (E2000) by RF (13.56 MHz) magnetron sputtering (Mirae Hi-tech Co., Ltd.) using high-density ceramic sintered ZIO targets with various In₂O₃ contents (In₂O₃ : 3.33, 6.50, 9.54, 12.44, 15.22 wt%; Samsung Corning Precision Glass Co., Ltd.). All of the deposition experiments were performed at room temperature (RT) under a pure argon atmosphere. The total gas

*Corresponding author. E-mail : pksong@pusan.ac.kr

pressure (P_{tot}) and RF power were varied in the ranges of 0.6-1.2 Pa and 60-120 W, respectively. The partial pressure of water in the residual gas and the substrate to target distance were maintained to be less than 1.33×10^{-3} Pa and 50 mm, respectively. Throughout the experiments, the ZIO targets were pre-sputtered for 10 min at an RF power of 100W to eliminate the impurities and obtain stable plasma on the target surface prior to deposition. The film thickness was measured using a reflectometer (ST2000-DLXn, K-MAC). The resistivity, Hall mobility and carrier density were estimated by Hall Effect measurements using the van der Pauw method (HMS-3000, Ecopia). The microstructure and optical transmittance were measured using X-ray diffraction (XRD) with $\text{CuK}\alpha$ (0.154 nm) radiation (D8 advance, Bruker) and UV spectroscopy (UV-1800, Shimadzu).

3. Results and Discussion

The optimum In_2O_3 doping ratio of the ZIO film obtained in our previous work was 9.54 wt% at RT by DC magnetron sputtering. Fig. 1 shows the variation in the electrical properties of the ZIO films with the (a) RF power and (b) working pressure. Especially, the RF power has a significant influence on the resistivity of the ZIO films. Fig. 2 shows the

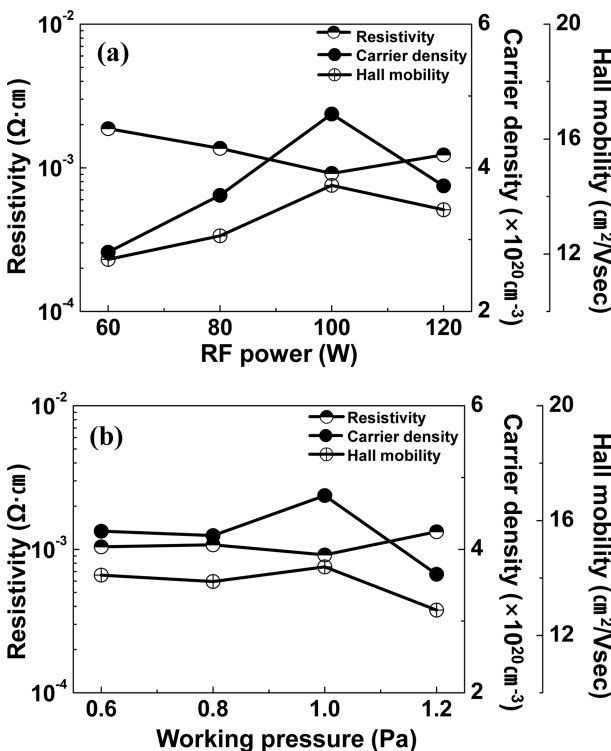


Fig. 1. Variation in electrical properties of ZIO films with (a) RF power, (b) working pressure.

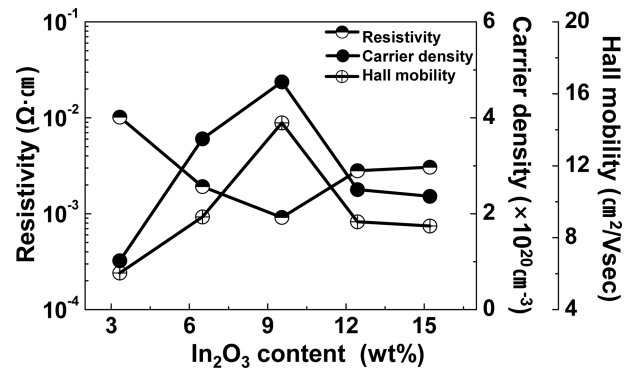


Fig. 2. The dependence of the electrical properties (resistivity, Hall mobility and carrier density) of the ZIO films on the In_2O_3 doping ratio.

dependence of the electrical properties (resistivity, carrier density and Hall mobility) of the ZIO films on the In_2O_3 content for the five different In_2O_3 doping ratios. The resistivity was found to decrease from 1.02×10^{-2} to 9.13×10^{-4} Ωcm as the In_2O_3 content was increased from 3.33 to 9.54 wt%, which was attributed to the significant increase of the carrier density from 1.02×10^{20} to $4.75 \times 10^{20} \text{ cm}^{-3}$. This initial increase in the carrier density of the ZIO films was due to the substitutional incorporation of In^{3+} ions into the Zn^{2+} sites⁶⁾. Thus, one free electron was produced by the replacement of one Zn atom. However, the resistivity of the ZIO films gradually increased as the In_2O_3 content was further increased up to 15.22 wt%. When the In_2O_3 content in the target was greater than 9.54 wt%, the carrier density decreased, because the increasing number of dopant In atoms form some kind of neutral defects and these neutralized In atoms do not contribute any free electrons⁷⁾. In addition, the Hall mobility also decreased as the In_2O_3 content was increased from 9.54 to 15.22 wt%, which was mainly affected by grain boundary scattering. This phenomenon will be discussed in detail in relation to the grain size of the ZIO films. Normally, the decrease of the mobility with increasing impurity content is ascribed to not only the dependence of the ionized impurity scattering on the carrier concentration, but also to the enhancement of the grain boundary scattering resulting from the disorder introduced into the ZnO lattice⁸⁾.

Fig. 3(a) shows the XRD patterns of the ZIO films for the five different In_2O_3 doping ratios. They were polycrystalline with a hexagonal structure and had a preferred orientation with the c-axis perpendicular to the substrate. No peak related to In_2O_3 was found,

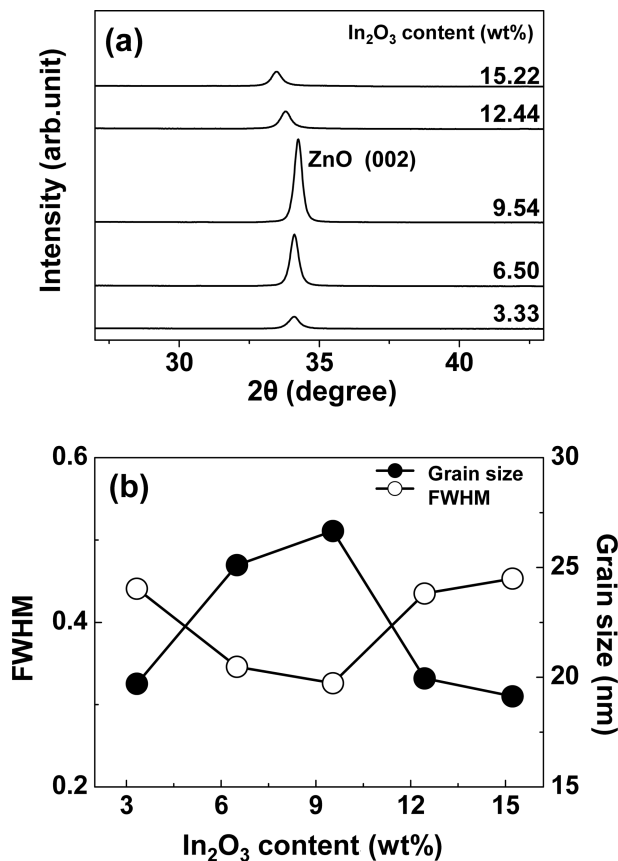


Fig. 3. (a) XRD patterns, (b) FWHM and grain size for the five different In₂O₃ doping ratios.

which indicated that most of the In atoms substitute for Zn in the hexagonal lattice and that the excess In atoms might occupy the interstitial sites of ZnO⁹⁾. The (002) peak intensity of the ZIO films increased significantly with increasing In₂O₃ content from 3.33 to 9.54 wt%. In general, films generally grow to minimize their surface free energy, which means that the (002) plane of the present films has the lowest density of surface energy¹⁰⁾. From these results, we considered that as the In₂O₃ content increased, the surface energy of the (002) plane was reduced and the migration of the sputtered atoms was enhanced by the sputtered In atoms which might act as a surfactant. However, the (002) peak intensity decreased dramatically with increasing In₂O₃ content. In addition, as the In₂O₃ content was increased up to 15.22 wt% in the ZIO films, their (002) diffraction peak shifted towards a lower angle. From these results, it can be inferred that more In³⁺ ions occupied the interstitial positions of the ZnO matrix, so that the lattice parameter of the c-axis increased with increasing In₂O₃ content¹¹⁾. It can also be understood that the decrease of the diffraction angle, θ , resulted in an increase of the lattice constant by Bragg's law. Fig. 3

(b) shows the FWHM and grain size of the ZIO films for the five different In₂O₃ doping ratios. To assess the quality of the ZIO films, the FWHM and grain size were used according to the Scherrer formula¹²⁾

$$D = B\lambda / \Delta\theta \cos\theta_B$$

where D is the grain size, B is a constant, $\Delta\theta$ is the FWHM, and θ_B is the Bragg angle. The film deposited at an In₂O₃ content of 9.54 wt% had the narrowest FWHM and the largest grain size. As shown in Fig. 3(b), the grain size was found to be between 18.21 to 26.66 nm. This can be explained by considering that the enhancement of the crystallinity increasing In₂O₃ content from 3.33 to 9.54 wt%. Therefore, the ZIO films with an In₂O₃ content of 9.54 wt% had the best structural properties. However, as the In₂O₃ content further increased, the grain size decreased, resulting in the deterioration of the crystallinity of the ZIO films. This might be due to the formation of compressive stresses caused by the occupancy of the In ions in the interstitial sites of the ZnO matrix, with the result that the excess In atoms prefer to cluster into the grain boundaries. This would cause crystal disorder and the consequent decrease of the grain size. This indicates that the increased resistivity of the ZIO films was due to the decrease of the mobility.

Fig. 4 shows the transmittance of the ZIO films in the wavelength range from 190 to 1100 nm for the five different In₂O₃ doping ratios. The average transmittance in the visible region was over 85% for all of the ZIO films using an air as a reference. At an In₂O₃ content of 9.54 wt%, the optical absorption edge shifted towards the shorter wavelength region.

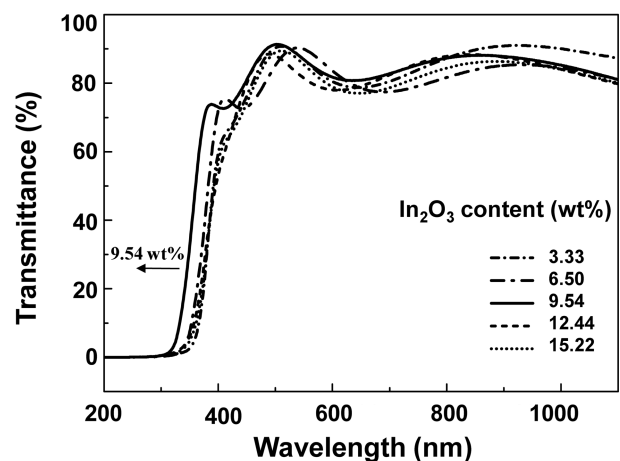


Fig. 4. The transmittance from 190 to 1100 nm of the ZIO films for the five different In₂O₃ doping ratios.

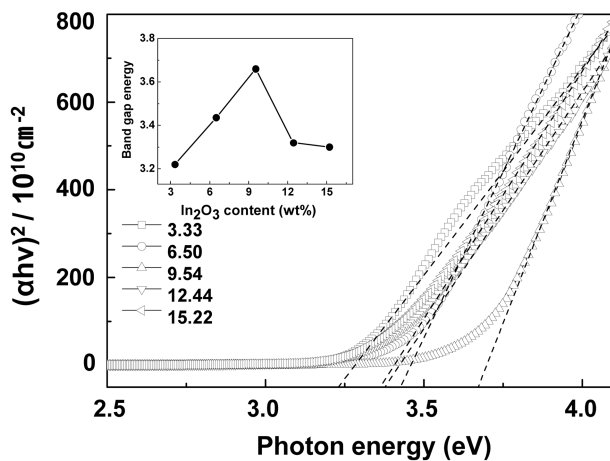


Fig. 5. Plot of absorption coefficient squared $(\alpha h\nu)^2$ versus photon energy (E_g) of the ZIO films for the five different In_2O_3 doping ratios.

This movement of the absorption edge to the shorter wavelength region is referred to as the Burstein-Moss shift, which is due to the increase in the carrier density¹³.

Fig. 5 shows the plot of the absorption coefficient squared $(\alpha h\nu)^2$ versus the photon energy (E_g) of the ZIO films for the five different In_2O_3 doping ratios. The absorption edge in the UV region was shifted gradually to a shorter wavelength. The adsorption coefficient (α) is calculated using the equation¹⁴

$$\alpha = -\ln(1/T)/d$$

where T and d are the transmittance and film thickness, respectively. The optical band gap dependence of the absorption coefficient is given by the following equation¹⁴

$$(\alpha h\nu)^2 = A(h\nu - E_g)$$

where A and α are constants for the direct transition and the optical absorption coefficient, respectively. The optical band gap (E_g) can be obtained by extrapolating the linear part of the curve resulting from this equation. The optical band gaps of the ZIO films deposited at In_2O_3 doping ratios of 3.33, 6.50, 9.54, 12.44, and 15.22 wt% were 3.22, 3.45, 3.66, 3.32, and 3.3 eV, respectively. This indicates that the optical band gap increased with increasing carrier density, which is indicative of the broadening of the optical band gap¹⁵. It is also known that ZIO films with a carrier density above 10^{20} cm^{-3} are degenerate and that the Fermi energy penetrates into the conduction band.

4. Conclusions

ZIO films were deposited using ZIO targets with five different In_2O_3 contents by RF magnetron sputtering. The dependence of the structural, electrical, and optical properties of the ZIO films on their doping content was investigated. The ZIO films deposited with an In_2O_3 content of 9.54 wt% showed the lowest resistivity of $9.13 \times 10^{-4} \Omega \text{ cm}$. All of the films were polycrystalline with a hexagonal structure and had a preferred orientation with the c -axis perpendicular to the substrate. The (002) peak intensity tended to increase as the In_2O_3 content in the ZIO targets was increased up to 9.54 wt%. The grain size and FWHM were found to be in the ranges of 18.21 to 26.66 nm and 0.326 to 0.453, respectively. The average transmittance in the visible region was over 85% for all of the ZIO films. The optical band gap increased with increasing carrier.

Acknowledgement

This work was supported for two years by Pusan National University Research Grant

References

1. P. Prathap, G. Gowri Devi, Y. P. V. Subbaiah, K. T. Ramakrishna Reddy, V. Ganesan, C. Appl. Phys., (2008) 8.
2. S. S. Lin, J. L. Huang, D. F. Lii, Mater. Chem. Phys., 90 (2005) 22.
3. S. H. Jeong, S. B. Lee, J. H. Boo, C. Appl. Phys., 4 (2004) 655.
4. S. H. Mohamed, A. M. Abd El-Rahman, A. M. Salem, L. Pichon, F. M. El-Hossary, J. Phys. Chem. Solids., 67 (2006) 2351.
5. M. Kon, P. K. Song, A. Mitsui, Y. Shigesato, Jpn. J. Appl. Phys., 41 (2002) 6174.
6. H. Kim, J. S. Horwitz, S. B. Qadri, D. B. Chrisey, Thin Solid Films., 420 (2002) 107.
7. G. K. Paul, S. Bandyopadhyay, S. K. Sen, S. Sen, Mater. Chem. Phys., 79 (2003) 71.
8. T. Minami, H. Sato, H. Nanto, S. Takata, Jpn. J. Appl. Phys., 24 (1985) 781.
9. Z. Q. Xu, H. Dong, J. Xie, Y. Li, X. T. Zu, Appl. Surf. Sci., 253 (2006) 476.
10. J. F. Chang, H. L. Wang, M. H. Hon, J. Cryst. Growth., 211 (2000) 93.
11. S. S. Lin, J. L. Huang, D. F. Lii, Surf. Coat. Technol., 176 (2004) 173.
12. M. Lv, X. Xiu, Z. Pang, Y. Dai, L. Ye, C. Cheng,

- S. Han, *Thin Solid Films.*, 516 (2008) 2017.
13. A. E. Manouni, F. J. Manjon, M. Mollar, B. Mari, R. Gomez, M. C. Lopez, J. R. Ramos-Barrado, *Superlattices and Microstructures*, 39 (2006) 185.
14. A. M. K. Dagamseh, B. Vet, F. D. Tichelaar, P. Sutta, M. Zeman, *Thin Solid Films*, 516 (2008) 7844.
15. G. Goncalves, E. Elangovan, P. Barquinha, L. Pereira, R. Martins, E. Fortunato, *Thin Solid Films*, 515 (2007) 8562.